NANO LETTERS

Letter

pubs.acs.org/NanoLett

Anisotropy of Excitation and Relaxation of Photogenerated Charge Carriers in Graphene

Martin Mittendorff,[*,†,‡] Torben Winzer,[§] Ermin Malic,[§] Andreas Knorr,[§] Claire Berger,[⊥,¶] Walter A. de Heer,[⊥] Harald Schneider,[†] Manfred Helm,[†,‡] and Stephan Winnerl[†]

[†]Helmholtz-Zentrum Dresden-Rossendorf, P.O. Box 510119, 01314 Dresden, Germany

[‡]Technische Universität Dresden, 01062 Dresden, Germany

[§]Technische Universität Berlin, Hardenbergstraße 36, 10623 Berlin, Germany

[⊥]Georgia Institute of Technology, Atlanta, Georgia 30332, United States

[¶]CNRS – Institut Néel, 38042 Grenoble, France

ABSTRACT: We present a pump–probe experiment on graphene, which reveals a pronounced dependence of the pump-induced transmission on the angle between pump and probe polarization. It reflects a strong anisotropy of the pump-induced occupation of photogenerated carriers in momentum space. Within 150 fs after excitation, an isotropic carrier distribution is established. The experiments are well described by microscopic modeling, which identifies carrier-phonon scattering to be the main relaxation mechanism giving rise to an isotropic carrier distribution.

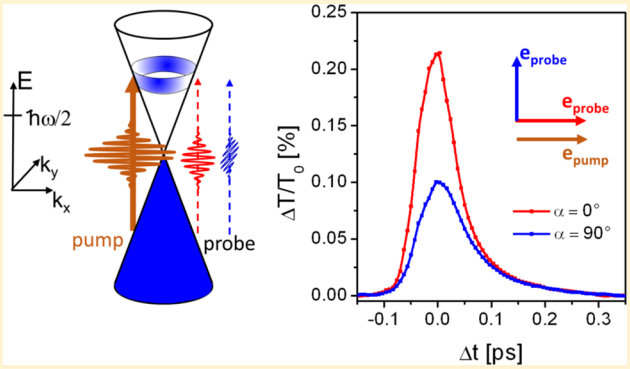

KEYWORDS: *graphene, carrier-dynamics, anisotropy, collinear scattering*

The peculiar band structure of graphene gives rise to a number of fascinating transport phenomena and optical effects.[1,2] Optical properties and carrier dynamics have been investigated on ultrashort time scales by pump–probe experiments involving photon energies from a few meV up to 5 eV.[3−11] The highest temporal resolution (below 10 fs) was reported for photon energies of 1.6 eV.[11] For photon energies above 2 eV, a deviation from linear dispersion and triangular warping of the band structure become important, whereas for smaller photon energies, the band structure is described in good approximation by an isotropic Dirac cone.[12] However, it has been shown theoretically that the polarization direction of linearly polarized radiation breaks the symmetry of the system.[13−15] The resulting distribution of photogenerated carriers exhibits maxima in the momentum directions perpendicular to the polarization direction and nodes in the directions parallel to the polarization direction. Such an anisotropic distribution of carriers generated by interband excitation is also expected for other materials. However, the complex structure of the valence bands in many materials results in an almost isotropic net distribution without nodes.[16] In graphene, on the other hand, the electron–hole symmetry makes the material ideally suited for studying the anisotropy of carrier excitation. Nevertheless, this effect has escaped experimental observation in pump–probe experiments so far, despite the large number of studies. Concerning the relaxation dynamics subsequent to optical excitation carrier–carrier and carrier–phonon contributions have been studied experimentally and theoretically.[3−10,14,15] For carrier–carrier scattering, it has been debated controversially how this process, which can satisfy energy and momentum conservation for two-particle interactions only in case of collinear scattering, can contribute to the carrier dynamics on the two-dimensional manifold of the band structure.[17−19] It has been predicted that interband carrier–carrier scattering, often called impact ionization or inverse Auger scattering, can result in carrier multiplication.[15,20] Evidence for this interesting effect has been obtained in a number of pump–probe experiments[8,19,21] and is a field of ongoing research. In two recent time- and angle-resolved photoemission spectroscopy studies, no indication for carrier multiplication has been observed.[22,23] However, this is consistent with theoretical predictions of the carrier multiplication.[20,24] At the applied pump fluences in the range of 1 mJ/cm^2 in refs 22 and 23, Auger recombination is the predominant scattering process, preventing carrier multiplication from occurring.

Our polarization-sensitive pump–probe experiments provide direct evidence for an anisotropic occupation. The carriers are generated by linearly polarized radiation of photon energy

Received: December 20, 2013
Revised: February 12, 2014
Published: February 21, 2014

ACS Publications © 2014 American Chemical Society

dx.doi.org/10.1021/nl404730y | *Nano Lett.* 2014, 14, 1504−1507

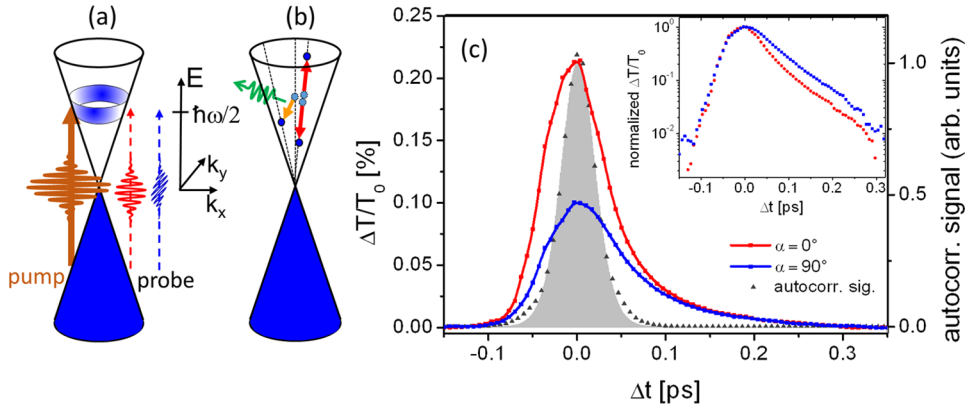

Figure 1. (a) Band structure of graphene with anisotropic conduction band occupation induced by a linearly polarized pump beam. (b) Illustration of collinear intraband carrier−carrier scattering preserving both energy and momentum. (c) Pump−probe signals for parallel polarization configuration ($\alpha = 0°$) and perpendicular polarization configuration ($\alpha = 90°$). The dots and squares are experimental data, and the lines are guides for the eye. The black triangles correspond to the measured autocorrelation signal; the gray shaded area is a fit to the autocorrelation data. For better comparison, the curves are shifted along the horizontal axis so that the maxima occur at $\Delta t = 0$. The inset depicts the same pump−probe data as in the main figure, but normalized and plotted on a logarithmic scale.

1.55 eV, that is, within the isotropic Dirac-cone region. An isotropic distribution is established within the first 150 fs after the optical excitation. It is reached by noncollinear scattering mainly mediated by optical phonons as unambiguously shown by our microscopic calculations. The faster decay component of the induced transmission observed for pump and probe beams with parallel polarization points toward strong collinear scattering preserving the initially generated anisotropic carrier distribution.

A Ti:sapphire laser served as a source for 30-fs pulses with a photon energy of 1.55 eV and a spectral width (full width at half-maximum fwhm) of 0.20 eV (repetition rate 78 MHz, pulse energy ∼3 nJ). The polarization of the pump pulses was varied by rotating a half-wave plate. The probe-beam path contained a second half-wave plate with fixed orientation; hence, both pump and probe pulses acquire equal amounts of dispersion. The stretching of the pulses by dispersion was partly compensated by introducing a down-chirp in front of the setup. An off-axis parabolic mirror focused both the pump and probe beam onto the sample under almost normal incidence. The applied pump fluence was 4 μJ/cm^2. The pulse duration at the sample position was characterized by quadratic autocorrelation with a β barium borate (BBO) crystal. The measured autocorrelation signal can be well described by a self-convolution of a sech^2 function with fwhm of 30 fs (cf. Figure 1). The pump-induced transmission change of graphene was recorded via lock-in detection based on modulation of the pump beam by a chopper. Scattered pump radiation was suppressed by spatial filtering in front of the photodetector. The experiments were performed at room temperature on two samples of epitaxial multilayer graphene (∼50 layers and ∼70 layers) grown by thermal decomposition of SiC on the C-terminated face of SiC.[25] Both samples showed similar effects; the data presented in this article stem from a sample with ∼50 graphene layers. The graphene-like nature of the layers was confirmed by Raman spectroscopy[26] and magnetospectroscopy.[27]

In Figure 1, the induced transmissions for parallel and perpendicular polarization orientation of pump and probe beam are presented. For the case of parallel polarization, the signal amplitude is slightly more than two times larger than for the case of perpendicular polarization. For time delays beyond 150 fs, no differences in the signals are found, indicating that an isotropic carrier distribution is reached on this time scale (cf. Figure 1c). For the configuration with perpendicular polarizations, a single-exponential decay with a time constant of 65 ± 5 fs was observed (cf. inset of Figure 1c). A similar decay occurs in the case of parallel polarization for delay times beyond 50 fs. For shorter delay times, however, a very fast initial decay is revealed (cf. inset of Figure 1c). The basically similar rise and fall time of the signal for parallel polarizations in the time interval [−50 fs, 50 fs] indicates that the fast decay is characterized by a time constant smaller than the pulse duration of 30 fs. The fact that this component is much faster than the time scale for establishing an isotropic distribution points toward pronounced collinear scattering, which preserves the initially anisotropic carrier distribution (cf. Figure 1b).

To study the anisotropy of the optical excitation in more detail, the angle α between pump and probe polarization was varied in steps of 10°. The measured amplitude of the signal follows a function $f(\alpha) = A_0 + A_1 \cos^2(\alpha)$ with $A_0 \approx A_1$ (cf. Figure 2). To verify that the anisotropy purely stems from the optical excitation, the sample was rotated and similar experiments were performed. No dependence of the pump−probe signals on sample orientation was found (not shown). The distribution of photogenerated carriers is determined by

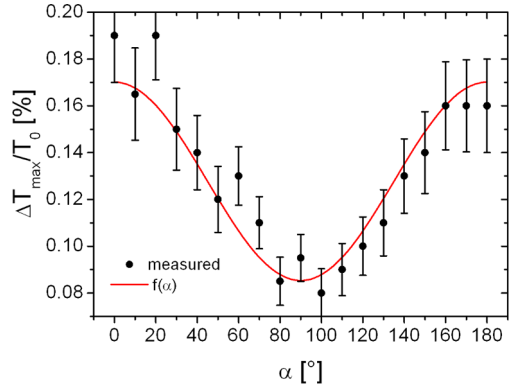

Figure 2. Dependence of the amplitude of the pump−probe signal on the angle α between pump and probe-beam polarization. The fit function $f(\alpha)$ is described in the main text.

dx.doi.org/10.1021/nl404730y | Nano Lett. 2014, 14, 1504−1507

the absolute square of the matrix element for the optical excitation, which is proportional to $|\sin \Phi_k|^2$.[13,14] The angle Φ_k is the angle between the momentum $\hbar\boldsymbol{k}$ of the photogenerated electrons in the conduction band and the polarization $\boldsymbol{P}$ of the radiation. Pauli blocking caused by pump-excited carriers is responsible for the induced transmission $\Delta T/T_0$. Taking into account the carrier distributions generated by the pump and probe beam, respectively, and integrating over Φ_k results in $\Delta T/T_0 \sim 1 + 2\cos^2(\alpha)$. This dependence is characterized by a maximum-to-minimum ratio of 3:1. The somewhat lower value of ~2:1 found in the experiment is a consequence of the finite temporal resolution of the experiment where carrier scattering occurs already during the excitation pulse. Note that even collinear scattering, which preserves the anisotropy of the carrier distribution, reduces the measured maximum-to-minimum ratio, as it scatters carriers out of the probed energy range.

Finally, we compare the experimental results with microscopic calculations based on the density matrix formalism. The carrier dynamics in the valence and conduction band is resolved in momentum, angle, and time.[14,15,28] Momentum-dependent rates for carrier−carrier and carrier−phonon scattering are microscopically obtained by applying the second-order Born−Markov approximation. The calculations are performed for excitation pulses with photon energy, pulse duration, and pump fluence like in the experiment. In Figure 3a, the carrier populations in the conduction band generated at $\Phi_k = 0°$ and $\Phi_k = 90°$, respectively, are compared. The initial population at $\Phi_k = 0°$ is zero, representing a node of the distribution. The population builds up due to noncollinear scattering. After 30 fs, the population decreases slowly, indicating that scattering out of this phase-space region dominates over in-scattering. In contrast, the population at $\Phi_k = 90°$ is initially strong and decreases successively. The calculated induced transmission is depicted in Figure 3b. In very good qualitative and quantitative agreement with the experiment, an amplitude ratio slightly above 2:1 is found for parallel and perpendicular polarization configuration. Also, the subsequent decay dynamics agrees very well with the experiment (cf. Figure 1c and 3b) considering that the modeling does not contain adjustable fitting parameters.

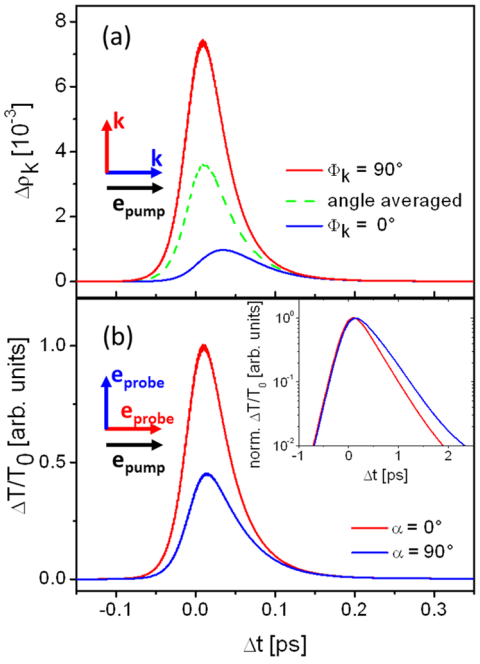

Figure 3. (a) Calculated pump-induced carrier occupation in the k-space regions corresponding to $\Phi_k = 0°$, $\Phi_k = 90°$ and averaged over all values of Φ_k. (b) Calculated pump-induced transmission for parallel polarization configuration ($\alpha = 0°$) and perpendicular polarization configuration ($\alpha = 90°$). The inset depicts the same pump−probe data as in the main figure, but normalized and plotted on a logarithmic scale.

Our calculations clearly show that intraband carrier−carrier scattering is the predominant collinear-scattering channel preserving the initial anisotropy. The main process resulting in an isotropic distribution, on the other hand, is found to be the scattering across the Dirac cone via optical phonons. A detailed analysis of the role of the different elementary processes in the relaxation dynamics is provided in ref 15.

When comparing the induced transmission for perpendicular polarizations with the population at $\Phi_k = 0$, a pronounced difference in the rise time stands out (cf. Figure 3a and Figure 3b). As discussed above, the population at $\Phi_k = 0$ builds up by scattering. In contrast, the induced transmission rises with a rate determined by the pump-pulse duration similarly to the induced transmission for the parallel polarization configuration. This similar rise is also found in the experiment. In the case of perpendicular polarizations, the rise is caused by the overlap of populations generated by pump and probe beams, in particular, in the phase-space regions around $\Phi_k = 45°$, 135°, 225°, and 315°.

We note that signatures of the optical anisotropy have been predicted[29,30] and observed[31] for photocurrents in electrically contacted graphene layers. In this case, an additional symmetry breaking is required, as the net momentum photocurrent is zero because positive and negative momentum distributions cancel each other. A bias field provides a preferred direction for the photocurrent. The anisotropy of measured photocurrents exhibits a maximum/minimum ratio of ~6:5. The lower value, as compared to that of our experiment, results from scattering, which contributes considerably stronger in the transport experiments. The anisotropic carrier excitation has also been studied in degenerate and two-color pump−probe experiments in a different geometry and with significantly lower temporal resolution (200 fs −300 fs) as compared to our experiment.[32,33]

Our findings have several interesting implications. First, pumping and probing with orthogonal polarization directions is often applied by experimentalists for purely technical reasons, namely in order to minimize the effects of scattered pump radiation. This technique has also been employed in a number of studies on graphene.[3,7,11] Our results show that this has no influence on the observed dynamics on time scales beyond 150 fs. On shorter time scales, however, one has to be aware that different relaxation dynamics are probed by the two polarization schemes. Second, the anisotropy in excitation and saturation may be exploited in all-optical switches that react differently to pulses of different polarization direction. Furthermore, the observation of the pronounced anisotropy in optical excitation will pave the way to experiments with more complex excitation conditions. In this respect $\omega-2\omega$−schemes have been proposed in theoretical studies,[34] where the distribution of excited carriers in k space can be controlled by varying the phase between the ω and 2ω pulse, giving rise to pure optical currents.[35]

In conclusion, a pronounced anisotropy in both the optical excitation and the subsequent ultrafast relaxation dynamics has

dx.doi.org/10.1021/nl404730y | Nano Lett. 2014, 14, 1504−1507

been revealed for electrons within the isotropic Dirac cone in graphene. The first effect is directly related to the anisotropy of the matrix elements for excitation with linearly polarized radiation. After 150 fs, an isotropic distribution is established. Furthermore, evidence is found for Coulomb-induced collinear scattering preserving the anisotropy on much shorter time scales. The results are expected to pave the way for interesting experiments based on optically controlled anisotropic effects in graphene.

AUTHOR INFORMATION

Corresponding Author

*M. Mittendorff. E-mail: m.mittendorff@hzdr.de. Phone: +49 351 260 3522. Fax: +49 351 260 3285.

Notes

The authors declare no competing financial interest.

ACKNOWLEDGMENTS

We acknowledge the financial support by the German Research Foundation (DFG) through SPP 1459. E.M. is grateful to the Einstein Foundation Berlin. S.W. is thankful for fruitful discussions with J. Rioux.

REFERENCES

(1) Geim, A. K; Novoselov, K. S. *Nat. Mater.* **2007**, *6*, 183−191.
(2) Bonaccorso, F.; Sun, Z.; Hasan, T.; Ferrari, A. C. *Nat. Photonics* **2010**, *4*, 611−622.
(3) Dawlaty, J. M.; Shivaraman, S.; Chandrashekhar, M.; Rana, F.; Spencer, M. G. *Appl. Phys. Lett.* **2008**, *92*, 042116.
(4) George, P. A.; Strait, J.; Dawlaty, J.; Shivaraman, S.; Chandrashekhar, M.; Rana, F.; Spencer, M. G. *Nano Lett.* **2008**, *8*, 4248−4251.
(5) Sun, D.; Wu, K.; Divin, C.; Li, X.; Berger, C.; de Heer, W. A.; First, P. N.; Norris, T. B. *Phys. Rev. Lett.* **2008**, *101*, 157402.
(6) Breusing, M.; Kuehn, S.; Winzer, T.; Malic, E.; Milde, F.; Severin, N.; Rabe, J. P.; Ropers, C.; Knorr, A.; Elsaesser, T. *Phys. Rev. B* **2011**, *83*, 153410.
(7) Winnerl, S.; Orlita, M.; Plochocka, P.; Kossacki, P.; Potemski, M.; Winzer, T.; Malic, E.; Knorr, A.; Sprinkle, M.; Berger, C.; de Heer, W. A.; Schneider, H.; Helm, M. *Phys. Rev. Lett.* **2011**, *107*, 237401.
(8) Tani, S.; Blanchard, F.; Tanaka, K. *Phys. Rev. Lett.* **2012**, *109*, 166603.
(9) Malard, L. M.; Mak, K. F.; Castro Neto, A. H.; Peres, N. M. R.; Heinz, T. F. *New J. Phys.* **2013**, *15*, 015009.
(10) Roberts, A. T.; Binder, R.; Kwong, N. H.; Golla, D.; Cormode, D.; LeRoy, B. J.; Everitt, H. O.; Sandhu, A. *arXiv.org, e-Print Arch., Condens. Matter* **2013**, *1310*, 2683.
(11) Breusing, M.; Ropers, C.; Elsaesser, T. *Phys. Rev. Lett.* **2009**, *102*, 086809.
(12) Castro Neto, A. H.; Guinea, F.; Peres, N. M. R.; Novoselov, K. S.; Geim, A. K. *Rev. Mod. Phys.* **2009**, *81*, 109−162.
(13) Grüneis, A.; Saito, R.; Samsonidze, G. G.; Kimura, T.; Pimenta, M. A.; Jorio, A.; Souza Filho, A. G.; Dresselhaus, G.; Dresselhaus, M. S. *Phys. Rev. B* **2003**, *67*, 165402.
(14) Malic, E.; Winzer, T.; Bobkin, E.; Knorr, A. *Phys. Rev. B* **2011**, *84*, 205406.
(15) Malic, E.; Winzer, T.; Knorr, A. *Appl. Phys. Lett.* **2012**, *101*, 221115.
(16) Rioux, J.; Sipe, J. E. *Phys. E (Amsterdam, Neth.)* **2012**, *45*, 1−15.
(17) Foster, M. S.; Aleiner, I. L. *Phys. Rev. B* **2009**, *79*, 085415.
(18) Otsuji, T.; Boubanga Tombet, S. A.; Satou, A.; Fukidome, H.; Suemitsu, M.; Sano, E.; Popov, V.; Ryzhii, M.; Ryzhii, V. *J. Phys. D: Appl. Phys.* **2012**, *45*, 303001.
(19) Brida, D.; Tomadin, A.; Manzoni, C.; Kim, Y. J.; Lombardo, A.; Milana, S.; Nair, R. R.; Novoselov, K. S.; Ferrari, A. C.; Cerullo, G.; Polini, M. *Nature Commun.* **2013**, *4*, 1987.
(20) Winzer, T.; Knorr, A.; Malic, E. *Nano Lett.* **2010**, *10*, 4839−4843.
(21) Tielrooij, K. J.; Song, J. C. W.; Jensen, S. A.; Centeno, A.; Pesquera, A.; Elorza, A. Z.; Bonn, M.; Levitov, L. S.; Koppens, F. H. L. *Nature Phys.* **2013**, *9*, 248−252.
(22) Gierz, I.; Petersen, J. C.; Mitrano, M.; Cacho, C.; Turcu, I. C. E.; Springate, E.; Stöhr, A.; Köhler, A.; Starke, U.; Cavalleri, A. *Nature Mat.* **2013**, *12*, 1119−1124.
(23) Johannsen, J. C.; Ulstrup, S.; Cilento, F.; Crepaldi, A.; Zacchigna, M.; Cacho, C.; Turcu, I. C. E.; Springate, E.; Fromm, F.; Raidel, C.; Seyller, T.; Parmigiani, F.; Hofmann, P. *Phys. Rev. Lett.* **2013**, *111*, 027403.
(24) Winzer, T.; Malic, E. *Phys. Rev. B* **2012**, *85*, 241404.
(25) Berger, C.; Song, Z.; Li, X.; Wu, X.; Brown, N.; Mayou, D.; Li, T.; Hass, J.; Marchenkov, A. N.; Conrad, E. H.; First, P. N.; de Heer, W. A. *Science* **2006**, *312*, 1191−1196.
(26) Ferrari, A. C.; Meyer, J. C.; Scardaci, V.; Casiraghi, C.; Lazzeri, M.; Mauri, F.; Piscanec, S.; Jiang, D.; Novoselov, K. S.; Roth, S.; Geim, A. K. *Phys. Rev. Lett.* **2006**, *97*, 187401.
(27) Sadowski, M. L.; Martinez, G.; Potemski, M.; Berger, C.; de Heer, W. A. *Phys. Rev. Lett.* **2006**, *97*, 266405.
(28) Malic, E.; Knorr, A. *Graphene and Carbon Nanotubes - Ultrafast Relaxation Dynamics and Optics*; Wiley-VCH: Weinheim, Germany, 2013.
(29) Mai, S.; Syzranov, S. V.; Efetov, K. B. *Phys. Rev. B* **2011**, *83*, 033401.
(30) Trushin, M.; Schliemann. *J. Euro. Phys. Lett.* **2011**, *96*, 37006.
(31) Kim, M.; Yoon, H. A.; Woo, S.; Yoon, D.; Lee, S. W.; Cheong, H. *Appl. Phys. Lett.* **2012**, *101*, 073103.
(32) Yan, X.-Q.; Liu, Z.-B.; Yao, J.; Zhao, X.; Chen, X.-D.; Kong, X.-T.; Xing, F.; Chen, Y.; Tian, J.-G. *arXiv* **2013**, *1301*, 1743.
(33) Yan, X.-Q.; Liu, Z.-B.; Yao, J.; Zhao, X.; Chen, X.-D.; Chen, Y.; Tian, J.-G. *arXiv* **2013**, *1312*, 6513.
(34) Rioux, J.; Burkhard, G.; Sipe, J. E. *Phys. Rev. B* **2011**, *83*, 195406.
(35) Sun, D.; Divin, C.; Mihnev, M.; Winzer, T.; Malic, E.; Knorr, A.; Sipe, J. E.; Berger, C.; de Heer, W. A.; First, P. N.; Norris, T. B. *New J. Phys.* **2012**, *14*, 105012.